Polymer 43 (2002) 2417–2424

polymer

www.elsevier.com/locate/polymer

Liquid crystalline (cyanoethylpropyl)cellulose and its optically anisotropic composites with acrylic polymers

Lidia Okrasa[a,*], Jacek Ulanski[a], Gisèle Boiteux[b]

[a]*Department of Molecular Physics, Faculty of Chemistry, Technical University of Lodz, ul. Zeromskiego 116, 90-924 Lodz, Poland*
[b]*Laboratoire des Matériaux Polymères et des Biomatériaux, UMR-CNRS 5627, Université 'Claude Bernard' Lyon 1, 43 Bd. du 11 Novembre 1918, 69622 Villeurbanne Cedex, France*

Received 8 October 2001; accepted 10 December 2001

Abstract

Described herein are anisotropic polymer composites, made up of (cyanoethylpropyl)cellulose (CEPC) and acrylic polymer. A band texture (which can be seen with a polarisation microscope) forms in CEPC and its lyotropic solutions in acrylic monomer after orientation as a result of relaxation phenomena. The photopolymerisation of acrylic monomer (acrylic or methacrylic acid) in an oriented lyotropic solution of CEPC 'freezes' the orientation, and stable birefringent polymer composites are created. Thermooptical analysis shows that these composites exhibit thermally reversible anisotropy of optical properties. Molecular relaxations in such composites were investigated by means of dielectric and mechanical spectroscopies. The molecular relaxation processes, characteristic of pure components, are preserved in these composites. Two representations were used in dielectric spectroscopy: the temperature dependences of dielectric loss ε'' and of electric modulus M''. The latter was especially useful in the high temperature range, where ionic conductivity dominates the dielectric response.

Keywords: (Cyanoethylpropyl)cellulose; Polymer composites; Molecular relaxations

1. Introduction

Since the first liquid crystal (LC) based on cellulose was reported by Werbowyj and Gray in 1976 [1], it has been discovered that cellulose and many of its derivatives can form the LC phase in concentrated solutions with the appropriate solvent (lyotropic LC), and sometimes in a liquid state without any solvent (thermotropic LC) as well. The cellulose derivatives (CD) often form the lyotropic phase in various vinyl solvents capable of polymerisation under UV light [2–5]. This makes a preparation of highly anisotropic composites possible with a 'frozen-in' mesophase by the photopolymerisation of the vinyl monomer in the mechanically oriented lyotropic mesophase [3–5]. (Cyanoethylpropyl)cellulose (CEPC) forms lyotropic solutions in acrylic acid (AA) as well as in methacrylic acid (MAA).

Other than by dynamic mechanical analysis, the relaxation behaviour of LC CD can be investigated by dielectric relaxation spectroscopy (DRS). Because of ionic conductivity [6,7], dielectric measurements of CEPC were limited until now to temperatures below or near the glass transition. The classical representation of dielectric relaxations, i.e. dielectric losses, can be used only when the ionic conductivity is low. At high temperatures, where ionic conductivity dominates, it is possible to detect the relaxation processes by analysing the electric modulus defined by Macedo et al. [8] ($M^* = 1/\varepsilon^*$). The real M' and imaginary M'' parts of the electric modulus can be calculated from ε' and ε'':

$$M' = \frac{\varepsilon'}{\varepsilon'^2 + \varepsilon''^2}; \qquad M'' = \frac{\varepsilon''}{\varepsilon'^2 + \varepsilon''^2}$$

Although permittivity representation is easier in an interpretation, modulus representation can be very useful where conductivity processes are involved [9–11].

In this paper, we present the morphology, thermooptical properties and molecular relaxations of CEPC and its composites with poly(AA) or poly(MAA). This study was performed by using optical microscopy, thermooptical analysis (TOA), dielectric spectroscopy and dynamic mechanical analysis.

2. Experimental

2.1. Materials

CEPC was obtained by the reaction of (hydroxypropyl)-cellulose (HPC) (Aldrich, MW = 100 000, MS = 3) and

---

[*] Corresponding author. Tel.: +48-42-631-3205; fax: +48-42-631-3218.
E-mail address: lokrasa@ck-sg.p.lodz.pl (L. Okrasa).

0032-3861/02/$ - see front matter © 2002 Elsevier Science Ltd. All rights reserved.
PII: S0032-3861(01)00811-4

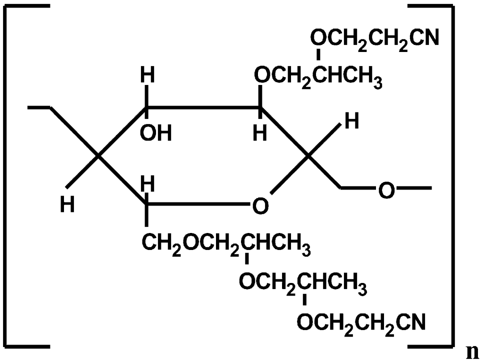

Fig. 1. Idealised structure of CEPC.

acrylonitrile [12]. The degree of substitution for cyanoethyl groups was about 2.8. The structure of CEPC is shown in Fig. 1. The samples for TOA and DRS studies were formed from the melt.

The CEPC/poly(AA) and CEPC/poly(MAA) composites were obtained by photopolymerisation of the acrylic monomer in the oriented solution of CEPC by a mercury lamp with a filter ($\lambda = 365$ nm) for 5 min. After polymerisation, the samples were annealed for 4 h at a temperature of 413 K. The orientation of the lyotropic LC solution of the CD prior to photopolymerisation was achieved by the mechanical shearing of a thin layer between two glass plates separated by the appropriate spacers. Three different compositions of each composite were prepared as follows: two in the mesophase range (60 and 40% of CEPC) and one below the critical concentration (20% of CEPC).

2.2. Measurements

TOA consists of recording the relative intensity of light transmitted through a sample placed under a microscope between crossed polarisers, I_T/I_1 (where I_T and I_1 are the intensities of the light at temperature T or at room temperature, respectively), as a function of temperature. TOA experiments were conducted in the temperature range 300–470 K using a Mettler FP 82 Microscope Hot Stage, and were performed for the sample orientation that yielded the highest transmission of polarised light, i.e. when the angle between the shearing direction of the sample and the polarisation plane of the polariser was about 45°. The heating rate was always 2 K/min.

DSC measurements were carried out using a 2920 TA Instrument or the Netzsch DSC 204. The samples were sealed in aluminium pans and measurements were performed with a heating rate of 10 K/min in an atmosphere of nitrogen. Before measurements, all samples were annealed at 413 K for 10 min.

Dynamic mechanical analyses (DMA) were carried out with a Dynamic Mechanical Thermal Analyzer Type DMA 2980 TA Instruments at fixed frequencies (1, 1.5, 5, 10, 30 Hz) with a heating rate of 2 K/min. The experiments were performed on the samples, which measured about $15 \times 5 \times 0.1\ \text{mm}^3$ under tension mode. The stress was applied parallel to the orientation direction of the samples.

DRS was performed in a Polymer Laboratories cell using the Hewlett Packard 4284A Precision LCR Meter at fixed frequencies in the 30 Hz–1 MHz range, and in the 210–460 K temperature range with a heating rate of 2 K/min. For the dielectric investigations, the 20 μm thick samples were prepared between two plates of conductive ITO glass with teflon spacers.

3. Results and discussion

3.1. Thermooptical behaviour and the morphology of CEPC systems

The unoriented sample of pure CEPC observed at room temperature under a microscope through crossed polarisers shows a grainy structure (see Fig. 2(a)), characteristic of cholesteric LCs. The behaviour of the unoriented samples of CEPC depends strongly on their thermal history. If the sample was annealed for a few minutes at 465 K (clearing temperature), and then quenched to room temperature, a very strong recrystallisation phenomenon was observed during subsequent heating. This process causes a very high increase of birefringence prior to isotropisation (see Figs. 2(b) and 3), and it is reversible during cooling. This phenomenon can be eliminated by long annealing at a temperature of 413 K. In this case, the sample has the same clearing temperature (465 K) as a sample that has not been annealed, but no increase of birefringence is observed prior to clearing, as shown in Fig. 3. After isotropisation, the samples of CEPC always return to a grainy structure during cooling.

In the oriented layer of CEPC, following the cessation of shearing, a texture evolution occurs and bands form perpendicular to the shearing direction [13]. The bands are distinct only under crossed polarisers; in non-polarised light the sample is clear and transparent in visible range. The brightness and darkness of the band varies with the angle between the shearing direction and the axis of the polariser. The intensity of light transmission is the strongest when this angle is 45° and the weakest when it is 0° and 90°, as shown in Fig. 4. The orientation of the CEPC sample is not stable; during heating it is destroyed and a grainy texture (much less birefringent) observed before shearing is recovered (Fig. 5(1c)). The decay of the orientation as temperature increases, detected by TOA, is shown on Fig. 6 (triangles).

Lyotropic solutions of CEPC in acrylic monomers also form band texture after shearing, but the orientation fades with time. The photopolymerised composite films have the same band texture (Fig. 5(2a)) as the solutions before polymerisation. The temperature dependencies of optical anisotropy in CEPC/poly(AA) and CEPC/poly(MAA) composites were also examined by means of TOA (Fig. 6).

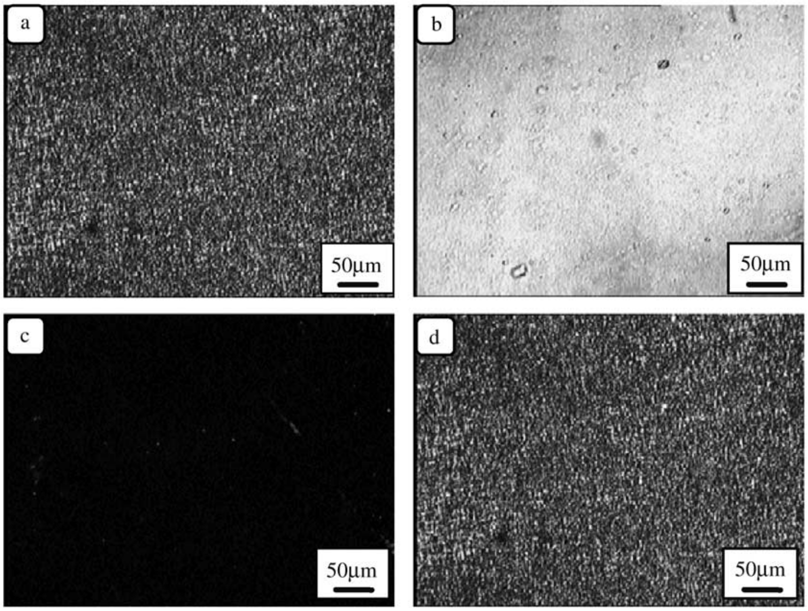

Fig. 2. Polarised micrographs of pure not oriented CEPC sample (20 μm thick layer annealed at 465 K for 5 min and then quenched to room temperature) registered during TOA at different temperatures: (a) 300, (b) 440, (c) 465 and (d) 300 K (after cooling), as marked in Fig. 3.

As opposed to thermotropic or lyotropic systems of CEPC, the band texture in the composites is stable in time and upon heating to isotropisation temperature that is characteristic of pure CEPC. The anisotropic optical properties for the composites are thermally reversible and the band texture recovers upon cooling, what is shown in Fig. 5(2c). The presence of polyacid reinforces the structure of the composites and acts as a 'memory factor' for the orientation of the polymer chains. One can see in Fig. 6 that in terms of the isotropisation temperature, there are no significant differences between composites with poly(AA) and poly(MAA). This is because both polyacids have a T_g below the isotropisation temperature of CEPC. However, one can see that in CEPC/poly(MAA) composites after isotropisation, the birefringence does not return to its original value. This is caused by the thermodegradation of the poly(MAA) component, which occurs above 460 K, while the thermodegradation of poly(AA) only begins above 490 K.

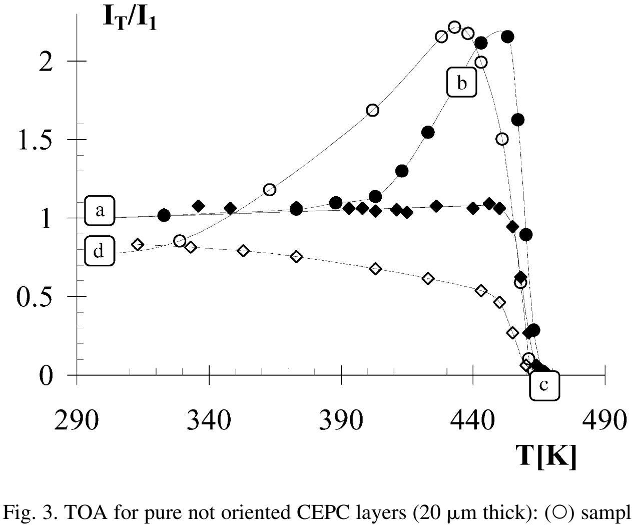

Fig. 3. TOA for pure not oriented CEPC layers (20 μm thick): (○) sample annealed at 465 K for 5 min and then quenched to room temperature, (◇) sample annealed at 413 K for 4 h (full symbols—heating, open symbols—cooling); (a), (b), (c) and (d) refer to micrographs shown in Fig. 2.

3.2. Molecular relaxation phenomena in CEPC systems

3.2.1. Dielectric relaxation spectroscopy

Glass transition phenomena: CEPC undergoes glass transition below room temperature (see Table 1). This phenomenon can be observed in dielectric spectroscopy as so-called α-relaxations [6]. Generally, it is assumed that the position of the maximum of the $\varepsilon''(T)$ plot coincides with the dynamic T_g, when the relaxation time τ is equal to 100 s. The values of T_g estimated by this method are shown in Table 1. The T_g value of pure CDs differs only slightly from the calorimetric values obtained using DSC. The T_g values from the DSC curves were determined as a midpoint.

The second component of the composites undergoes glass transition at a much higher temperature (poly(AA) at about 383 K, poly(MAA) at about 480 K). However, at lower temperatures both of them show β-relaxation processes, which are associated with local segment motions [6].

The dielectric constant values of the HPC derivatives strongly depend on the chemical structure of the side groups, and the dielectric strength ($\Delta\varepsilon$) reflect the polarity of the substituents [6]. Therefore, ε' and $\Delta\varepsilon$ obtained for the CEPC are high due to the presence of highly polar CN groups. The amplitude of the α-peak of CEPC is much stronger than the amplitude of the poly(AA) β-peak, which appears in the same temperature range. We assume that the α-relaxation of CEPC is preserved in the composites

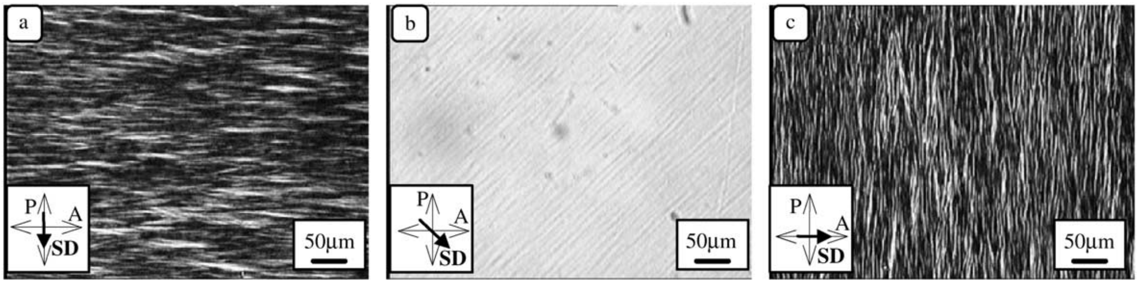

Fig. 4. Polarised micrographs of oriented CEPC layer at 300 K, with different angles between the shearing direction (SD) and the polarisation plane of the polariser (P): (a) 0°, (b) 45° and (c) 90°.

with poly(AA), and certain changes in the shape of the α-loss maximum are due to an overlap with the β-relaxation of poly(AA). Fig. 7 shows the temperature dependencies of dielectric permittivity (ε'), loss (ε'') and the imaginary part of the modulus (M'') at 1 kHz for the CEPC/poly(AA) composites in the low temperature range. We have found that the temperatures at which $M''(T)$ diagrams show maxima are lower (by ca. 2–20 K) in comparison to those for the $\varepsilon''(T)$ plots. The amplitudes of ε'' reflect the composition of the composites. Fig. 8(a) shows the Arrhenius diagrams for α-relaxation in pure CEPC and CEPC/poly(AA) composites. The character of these curves shows that they do not obey the Arrhenius law, what is to be expected of any α-relaxation process. One can see that the slopes of these curves decrease with the decreasing content of CEPC in the systems. A numerical analysis of the α-relaxations of different cellulose systems by means of the Williams–Landel–Ferry equation was already reported [6].

The values of T_g determined from the dielectric results slightly decrease with the decrease of CEPC concentration. Contrary to the DRS results, the values of the T_g temperatures of CEPC in the composites, obtained by means of DSC, are practically the same as that of pure CEPC (see Table 1). This indicates that the dielectric relaxation processes seen in the CEPC/poly(AA) composites are not pure α-relaxation of CEPC, but it overlaps with the β-relaxation of poly(AA). This effect is particularly strong in the CEPC/poly(AA) (20:80) composite. There is no clear α-maximum, but a broad band strongly influenced by the β-relaxation of poly(AA) is observed.

The α-relaxation of CEPC is also preserved in the composites with poly(MAA), and in this case one can also see certain changes of the loss maximum due to an overlap with the β-relaxation of poly(MAA), which occurs in the same temperature range. Fig. 8(b) shows the Arrhenius diagrams for α-relaxation in CEPC/poly(MAA) composites and in pure CEPC.

Transition phenomena associated with the formation of a mesophase: All dielectric relaxation phenomena are dominated by conduction phenomena at high temperatures, and it is only possible to detect the relaxation processes in

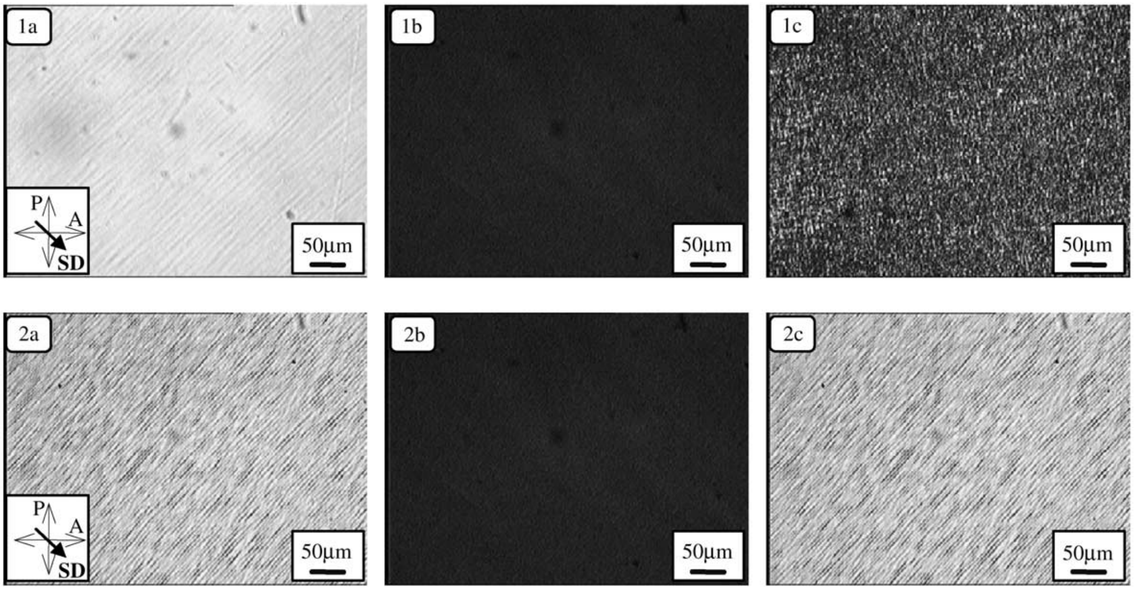

Fig. 5. Polarised micrographs for oriented (1) pure CEPC and (2) CEPC/poly(AA) (40:60) composite at different temperatures: (a) 300 K before heating, (b) 470 K and (c) 300 K after cooling.

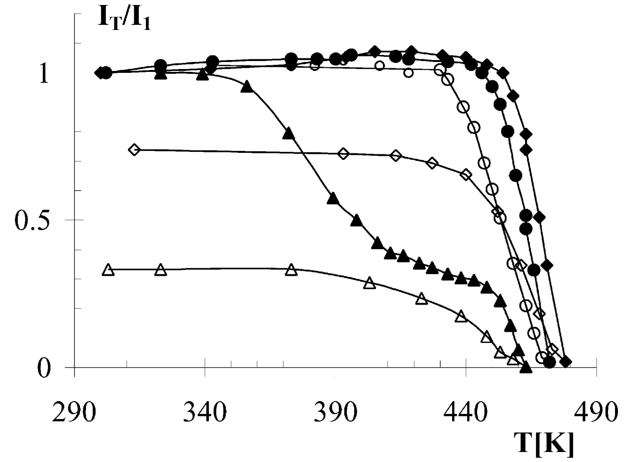

Fig. 6. TOA for oriented systems: (▲ △) pure CEPC, (● ○) CEPC/poly(AA) (40:60) and (◆ ◇) CEPC/poly(MAA) (40:60) composites (full symbols—heating, open symbols—cooling).

the dielectric spectra by an analysis of the electric modulus. The correlation between conductivity relaxations and molecular relaxations was reported earlier for other cellulose systems [10,11]. Fig. 9 shows the temperature dependencies of the electric modulus, which enable an indirect observation of the relaxation phenomena at a higher temperature. Fig. 10 shows the high temperature range of Arrhenius plots with data taken from the $M''(T)$ diagrams. In the $M''(T)$ diagram for pure CEPC, the second relaxation process appears at a temperature much above T_g. This conductivity relaxation is most probably stimulated by the so-called α'-relaxation, correlated with the transition from a frozen anisotropic phase to a mobile LC phase [10,11]. Unfortunately, the exact temperature of this transition for the investigated material is not known because it is not visible on the DSC curves. This transition is very rarely detected in this kind of LCs; on the other hand, it is evident that the liquid crystalline polymers transform into the mesophase somewhere in the temperature range between T_g and isotropisation temperature (T_i).

The α-relaxation associated with the glass transition can be seen in pure poly(AA) in a high temperature range. This process occurs at a higher temperature than the α'-relaxation of the CEPC sample. The α-relaxation of pure poly-(MAA) occurs at even higher temperatures ($T_g = 480$ K), ones above our investigation range. At such temperatures, poly(MAA) already undergoes thermal degradation.

Table 1
Glass transition temperatures determined from DSC and DRS measurements

Materials	T_g (K)	
	From DSC	From DRS
CEPC	255	254
CEPC/poly(AA) (60:40)	253	255
CEPC/poly(AA) (40:60)	254	251
CEPC/poly(AA) (20:80)	253	247

In the CEPC/poly(AA) composites the high temperature relaxation processes are seen as one broad peak occurring at intermediate temperatures in relation to the high temperature relaxation phenomena of pure components (Figs. 9(a) and 10(a)). In the composites with poly(MAA), the situation is similar (Figs. 9(b) and 10(b)); the high temperature relaxation phenomena occur in temperatures similar to those of composites with poly(AA). The fact that T_g temperatures of poly(AA) and poly(MAA) are different indicates that in both cases we see the α'-relaxation of CEPC shifted towards higher temperatures due to interactions with stiffer acrylic component.

3.2.2. Dynamic mechanical analysis

DMA is one of the methods that is sensitive to molecular motions in the materials. Transitions in the materials can be defined by the interpolated onset temperature of the $E'(T)$

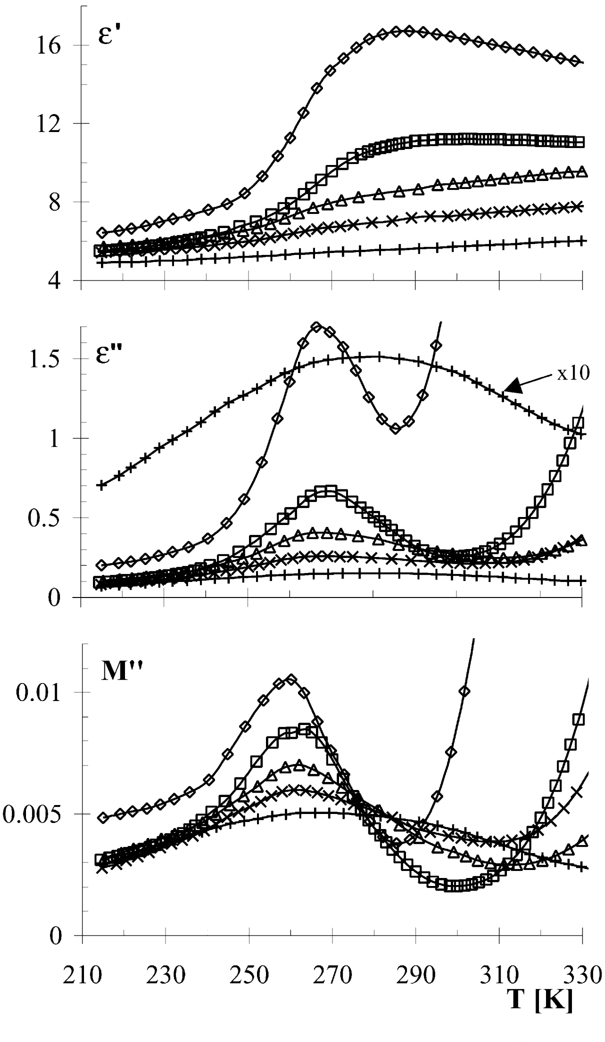

Fig. 7. Temperature dependencies of dielectric permittivity (ε'), dielectric loss (ε'') and electric modulus (M'') in the low temperature range at 1 kHz for the CEPC/poly(AA) composites with different compositions: (◇) pure CEPC, (□) 60:40, (△) 40:60, (×) 20:80 and (+) pure poly(AA).

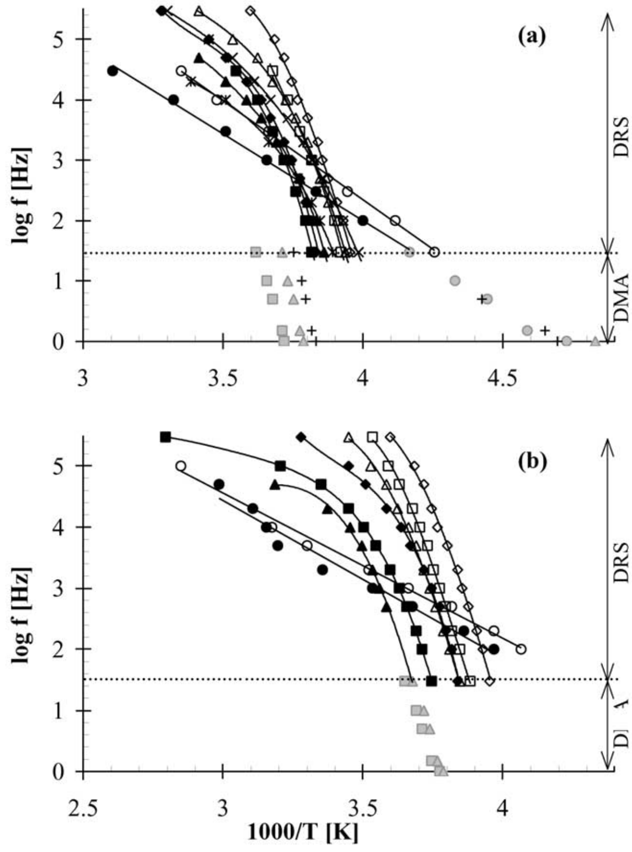

Fig. 8. Low temperature range of Arrhenius plots for (a) CEPC/poly(AA) and (b) CEPC/poly(MAA) composites with different compositions: (◇ ◆) pure CEPC, (□ ■ ▨) 60:40, (△ ▲ ◬) 40:60, (× ✱ +) 20:80 and (○ ● ◉) pure poly(AA) or poly(MAA). The points are taken from the $\varepsilon''(T)$ (◆ ■ ▲ ✱ ●), $M''(T)$ (◇ □ △ × ○) and $E''(T)$ (▨ ◬ + ◉) diagrams.

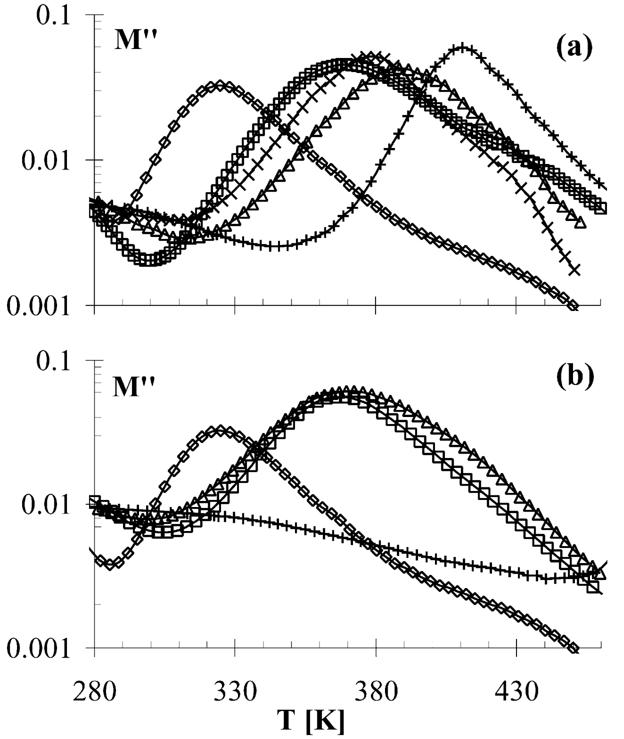

Fig. 9. Temperature dependencies of electric modulus (M'') at 1 kHz for (a) CEPC/poly(AA) and (b) CEPC/poly(MAA) systems with different compositions: (◇) pure CEPC, (□) 60:40, (△) 40:60, (×) 20:80 and (+) pure poly(AA) or poly(MAA).

plot, or by the maximum relaxation temperatures in the $E''(T)$ or tan $\delta(T)$ curves. In the present study, peak temperatures of the $E''(T)$ curves were generally used. There was an exception made in the case of CEPC/poly(MAA) composites, for which the peak temperatures in the tan $\delta(T)$ curves were used because of difficulties in determining the temperature maxima in the $E''(T)$ curves.

Fig. 11 shows the temperature dependencies of the storage modulus, loss modulus and loss tangent for CEPC/poly(AA) systems with different concentrations. Pure poly(AA) shows two relaxation processes in DMA, similar to those in DRS: the first one is connected with side-group motions (β-relaxation) and the second one is associated with the onset of large-scale motion of molecular chain segments—T_g phenomenon (α-relaxation). Their locations on the $E''(T)$ plot indicate very good agreement with the dielectric results for the β-relaxation (Fig. 8(a)), but are slightly shifted to higher temperatures for the α-relaxation (Figs. 8(a) and 10(a)). Unfortunately, it was not possible to take the DMA measurements for pure poly(MAA) using the accessible apparatus because of the high fragility of the poly(MAA) films.

In the composites, three transitions are apparent in the $E''(T)$ curves. They can be identified as the β-relaxation of poly(AA), the α-relaxation of CEPC and the α-relaxation of poly(AA) in order to the increasing temperature at which they appear. The first transition, the β-peak of poly(AA), is strongly masked in the CEPC/poly(AA) composites. This results from the fact that the α-relaxation process of this CD is very strong and it dominates in this temperature range, even for the 20:80 composition. The determination of the temperatures at which the β-peaks of poly(AA) appear in the $E''(T)$ curves was possible only for the lowest frequencies. The second relaxation process, called α, is related to CEPC and corresponds well to its glass transition. This process is shifted to a slightly higher temperature as compared to the dielectric spectroscopy results (Fig. 8(a)), however, the slopes of the Arrhenius plots agree with those obtained from the dielectric spectroscopy. The third high temperature relaxation in the composites is due to the α-relaxation process of poly(AA). In composites with 60 or 40 wt% of CEPC, this peak is not clearly visible on the $E''(T)$ plot and a more detailed examination was not possible. For the lowest content of CEPC, this peak can be distinguished and its temperature dependence is shown on the Arrhenius plots in Fig. 10(a). The position of this relaxation is close to the α-peak position for pure poly(AA). This relaxation was not visible in the DRS spectra. On the other hand, the DRS results of the CEPC/poly(AA) composite show the α′-relaxation of CEPC. This relaxation of

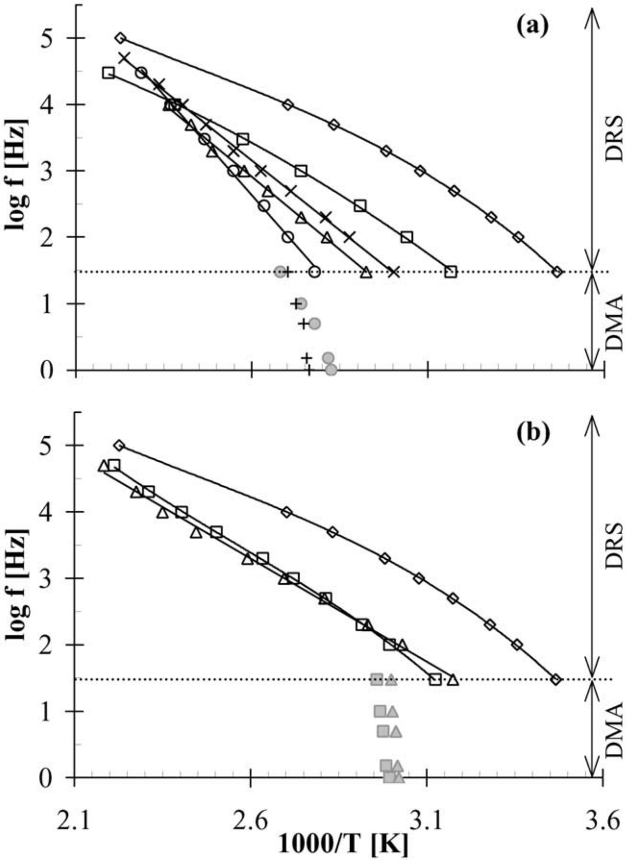

Fig. 10. High temperature range of Arrhenius plots for (a) CEPC/poly(AA) and (b) CEPC/poly(MAA) composites with different compositions: (◇) pure CEPC, (□ ▨) 60:40, (△ ▲) 40:60, (× +) 20:80 and (○ ●) pure poly(AA) or poly(MAA). The points are taken from the dielectric $M''(T)$ (◇ □ △ × ○) and mechanical $E''(T)$ (a) or tan $\delta(T)$ (b) (▨ ▲ + ●) diagrams.

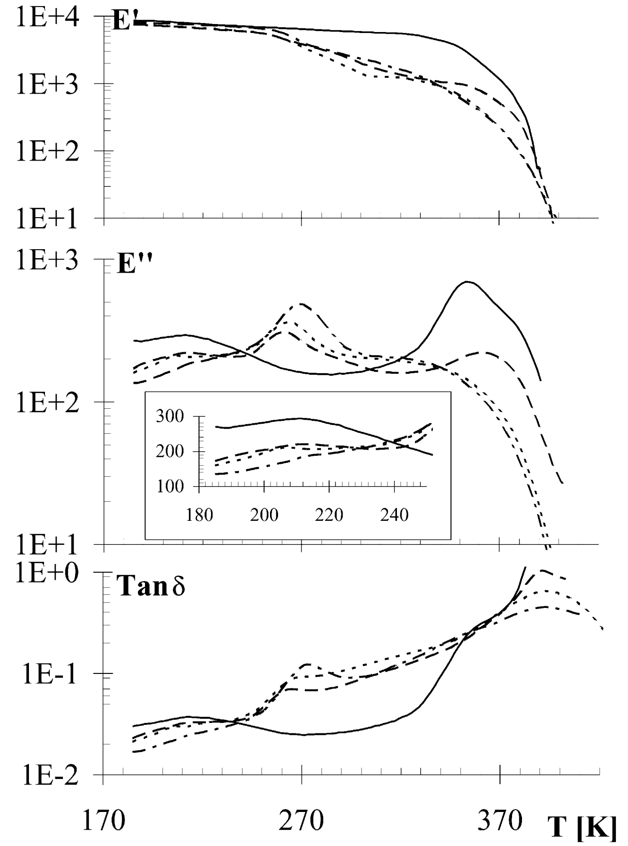

Fig. 11. Temperature dependencies of storage modulus (E'), loss modulus (E'') and loss tangent (tan δ) at 1 Hz of the CEPC/poly(AA) composites with different concentrations: (–·–·–) 60:40, (···) 40:60, (– – –) 20:80 and (—) pure poly(AA).

CEPC is not visible in the DMA spectra, perhaps because it is masked by the much stronger α-relaxation of poly(AA).

The DMA results of the CEPC/poly(MAA) composites are more difficult to analyse. Only the α-relaxation of CEPC is clearly visible, similar to that in composites with poly(AA) (Fig. 8(b)). The β-relaxation of poly(MAA) is almost invisible. The α′-relaxation of CEPC and the α-relaxation of poly(MAA) are only marked on the $E''(T)$ curves and it is practically impossible to examine them. On the tan $\delta(T)$ curves, only the α′-relaxation of CEPC is visible enough for analysis in terms of Arrhenius plots (Fig. 10(b)). These plots do not coincide well with the dielectric results, but one should take into account that the tan $\delta(T)$ maxima always appear at higher temperatures in comparison with the $E''(T)$ curves.

4. Conclusions

The photopolymerisation of oriented lyotropic solutions of CEPC in polymerisable solvents (poly(AA) or poly(MAA)) yields anisotropic polymer composites. A very interesting characteristic of such composites is the reversibility of their optical anisotropy. Contrary to oriented pure thermotropic CEPC, the anisotropic band texture and optical anisotropy reappear during cooling after isotropisation in the form that they were in before heating. This is most probably caused by the fact that the orientation of the CEPC component in lyotropic solution induces the orientation of growing polyacid chains during photopolymerisation, so that the formed polyacid network is anisotropic as a whole with elongated nano-niches containing cellulosic components. After isotropisation such oriented polyacid macromolecules (or an anisotropic polyacid network) can induce the reorientation of the CD component.

Three relaxation phenomena occur in CEPC when temperature increases: the glass transition of an amorphous phase, the transition from the anisotropic phase to a mobile mesophase and the transition from the mesophase to isotropic liquid. The second component has two characteristic relaxations: β associated with local movement and α associated with its glass transition. In the composites one can see the relaxation phenomena of both components, although they are more or less modified. A comparison of the DRS and DMA results shows that electric modulus representation can be a very useful tool in investigations of relaxation phenomena, especially in systems with high ionic conductivity. It can be used to detect the so-called α'-relaxation in particular, which is related to the transition from the frozen anisotropic phase to a mobile liquid crystalline phase, and which is usually difficult to detect using other methods.

Acknowledgements

We would like to thank Dr Gerard Seytre (UCB, Lyon) for his continuous help in dielectric studies, Dr Piotr Wojciechowski (TUL, Lodz) and Dr Andreas Schönhals (BAM, Berlin) for fruitful discussion. This work was partially supported by grant KBN No. 7 T08A 01320.

References

[1] Werbowyj RS, Gray DG. Mol Cryst Liq Cryst 1976;34:97.
[2] Gray DG. J Appl Polym Sci: Appl Polym Symp 1983;37:179–92.
[3] Ulanski J, Wojciechowski P, Kryszewski M. Nonlinear Optics 1995;9:203–11.
[4] Wojciechowski P, Ulanski J, Kryszewski M, Okrasa L, Czajkowski W. SPIE 1995;2372:268–74.
[5] Wojciechowski P, Okrasa L, Ulanski J, Kryszewski M. Adv Mater Opt Electron 1996;6:383–6.
[6] Okrasa L, Ulanski J, Wojciechowski P, Boiteux G, Seytre G. J Non-Cryst Solids 1998;235–237:658–63.
[7] Sato T, Tsujii Y, Kita Y, Fukuda T, Miyamoto T. Macromolecules 1991;24:4691–7.
[8] Macedo PB, Moynihan CT, Bose R. Phys Chem Glasses 1972;13:171.
[9] Mertens IJA, Wübbenhorst M, Oosterbaan WD, Jenneskens LW, van Turnhout J. Macromolecules 1999;32:3314–24.
[10] Okrasa L, Boiteux G, Ulanski J, Seytre G. Mater Res Innovat 2001;4:278–83.
[11] Okrasa L, Boiteux G, Ulanski J, Seytre G. Polymer 2001;42:3817–25.
[12] Mays JW. Macromolecules 1988;21:3179–83.
[13] Wojciechowski P. Mol Phys Rep 1999;25:64–71.